HYDROGEN DIFFUSION NEAR A CRACK TIP AFTER CYCLIC LOADING IN A STRAIN-HARDENING MATERIAL

J. Toribio and V. Kharin
Department of Materials Engineering, University of Salamanca
E.P.S., Campus Viriato, Avda. Requejo 33, 49022 Zamora, Spain
Tel: (34-980) 54 50 00; Fax: (34-980) 54 50 02, E-mail: toribio@usal.es

Abstract

A coupled quantitative modelling is performed of the large-deformation elastoplastic stress-strain field and transient stress-assisted diffusion of hydrogen near a pre-fatigued crack in a strain-hardening material under dynamic loading. As a consequence of the formation of the localised shear bands near the crack tip, separate locations of possible hydrogen assisted microfracture nuclei are specified: one associated with the maximum tensile stress, and the other related to the plastic strain concentration in the shear bands. Comparison of hydrogen diffusion to these sites under sustained and dynamic loadings shows that the latter one may promote earlier initiation of hydrogen assisted fracture under substantial participation of the strain factor in microscopic fracture mode.

Introduction

Advancement of hydrogen assisted cracking (HAC) in metals is limited by hydrogen supply to local rupture sites. Hydrogen diffusion affected by the stress-strain state has been proposed and substantiated as the transport mode able to control the kinetics of HAC (Van Leeuwen [1], Toribio and Kharin [2,3]). Analysis of hydrogen accumulation in the crack tip region has received much attention ([1-3], Sofronis and McMeeking [4], Toribio and Kharin [5]). However, a void has been left with regard to the combined effect on HAC of the crack history (residual stress-strain field), applied load dynamics under HAC conditions, and strain-hardening constitutive behaviour of common materials. This paper attempts to couple these variables which, in particular, seem to be important in the assessment of the alternative testing techniques aiming to evaluate material susceptibility to HAC — the sustained and rising load tests — as well as in a judgement about the factors which can promote hydrogen induced failures in service.

Model outline

The basic idea about HAC states that local fracture event in a material cell near the crack tip is determined by a critical combination of hydrogen concentration C and of stress-strain state [1-3]. Thus, a critical concentration C_{cr} exists as a function of responsible characteristics of the stress and strain therein, the maximal principal stress σ_1 and the equivalent plastic strain ε_{eq}^p, for definiteness [2,3]. HAC starts at time t when the concentration of hydrogen reaches this critical value in a relevant material unit at a certain location x_c:

$$C(x_c,t) = C_{cr}\left(\sigma_1(x_c,t),\ \varepsilon_{eq}^p(x_c,t)\right) \qquad (1)$$

Hydrogen supply to rupture sites in metals proceeds by diffusion driven by stresses and plastic strains [1-5]. Confining only to the role of stress, the equation of hydrogen diffusion in

the deformed configuration of a medium is reduced to the following ([4,5], Toribio and Kharin [6]):

$$\mathbf{Fel!} = -\nabla \bullet D\ \mathbf{Fel!} \qquad (2)$$

where D is the diffusion coefficient, V_H the partial molar volume of hydrogen in metal, R the universal gas constant, T the absolute temperature, and σ the hydrostatic stress.

For certain cases the entry conditions for hydrogen into metal correspond to the equilibrium on the material-environment interface, so that the boundary condition for diffusion takes the form [2,3]:

$$C\ (\text{at } x = 0) = C_0 \exp \mathbf{Fel!} \qquad (3)$$

where x is the coordinate axis which has the origin on the crack tip contour and crosses the metal beyond the tip, and C_0 represents the environmental hydrogen activity [2,3]. Material is considered to be hydrogen-free as the initial condition for diffusion.

As a prototype for simulations, a cold-drawn high-strength pearlitic steel is used, for which ample experimental study of the susceptibility to HAC has been performed (Toribio and Lancha [7]). Its characteristics are as follows: Young modulus E = 195 GPa, Poisson ratio $\mu = 0.3$, the value of 0.2% offset yield strength taken as the initial tensile yield stress σ_Y = 1500 MPa, and fracture toughness K_{IC} = 84 MPa·m$^{1/2}$. The strain-hardening behaviour described elsewhere [7] is approximated by the Ramberg-Osgood equation in terms of the equivalent plastic strain ε_{eq}^p and the equivalent stress σ_{eq} (in MPa) as $\varepsilon_{eq}^p = (\sigma_{eq}/2160)^{17}$. Material is considered to be rate-independent elastoplastic with von Mises yield surface and combined isotropic-kinematic hardening rule. This choice is determined by two reasons: the first is that the kinematic-type hardening is expected to be more suitable to bring out peculiar features of the stress-strain state generated by fatigue pre-cracking (e.g., those associated with the Bauschinger effect), the other is that pure kinematic hardening promoted strain localisation near the crack tip which made difficult to terminate simulations because of degeneration of the deformed finite element mesh. Thus, combined hardening is adopted as a compromise. Hydrogen-related material parameters are taken typical for steels [1-5], such as $V_H = 2 \cdot 10^{-6}$ m^3/mol and $D = 10^{-13}$ m^2/s at ambient temperature T = 293 K.

As a model, plane-strain double-edge-cracked panel under remote tension, the same as used in other studies ([5,6]), is considered. In particular, the width of the initial parallel-flanks crack (twice its semicircular tip radius) is $b_0 = 5$ μm. The small-scale yielding in the fracture mechanics sense [2,3,6] is ensured there, so that the stress intensity factor K is used as the controlling mechanical variable.

According to the experiments [7], the simulated loading histories consisted of the pre-cracking by zero-to-tension fatigue load with the maximum stress intensity factor $K_{max} = 0.6K_{IC}$ before HAC, followed by the rising load HAC test with constant stress intensity factor rate $dK/dt = K^{\bullet}$. Diffusion computations were carried out for $K^{\bullet} = 0.15$ and 1.5 MPa·m$^{1/2}$/min. The candidate (reference) value of the stress intensity factor for HAC initiation in simulations was taken $K_R = 1.3K_{max}$.

Large deformations of a solid are essential for near-tip diffusion since they not only affect the stress-strain state , but also change the diffusion distances in the crack tip zone [4-6]. The nonlinear finite element code *MARC* was employed to solve the mechanical portion of the coupled problem of stress-assisted diffusion with updated Lagrangian description of the deformed medium. Implementation of the diffusion initial-boundary value problem (2)-(3) in

material coordinates is described elsewhere [6]. Peculiarities of the finite-element solution procedure are basically the same as before dealing with a perfectly plastic material [5,6].

Results and analysis

Distributions of the maximum principal stress σ_1 and the equivalent plastic strain ε_{eq}^p which govern local fracture criterion (1), and of the hydrostatic stress which drives hydrogen diffusion according to equations (2)-(3) are the key items for HAC. Depending on the material, the stress-strain state, and the distribution of hydrogen (which together govern the fracture micromechanism), the respective fracture criterion (1) may become predominantly stress- or strain-controlled (Kharin [8], Panasyuk and Kharin [9]). This is especially proper for local hydrogen assisted fracture near the crack tip, where steep extrema of tensile stress and plastic strain are separated, and hydrogen distribution is usually inhomogeneous [3-6,9]. All these factors add ambiguity with regard to the definition of the critical cell location x_c. Meanwhile, since it is the hydrogen transportation distance, this is important for the interrelations between hydrogen transport and HAC kinetics.

Incorporation of the strain-hardening constitutive behaviour in modelling brings more insight about the crack tip mechanics. The data about stress-strain state near the crack tip during monotonic loading HAC test after fatigue pre-cracking are illustrated in Fig. 1 for the load level K_R which for the modelling purposes is considered to be a candidate for HAC initiation. The most notable finding is the development of the localised shear bands (Fig. 1) which is created by the kinematic component of the strain hardening. Plastic strain localisation affects the stress distributions (Fig. 1) comparing with a perfectly plastic material considered earlier [5,6]. This implies two potential sites of the microfracture initiation near the crack tip. The first one is associated with the local peak of plastic strain situated at $x_{c\varepsilon}$ (Fig. 1) and relies on strain-controlled fracture micromechanism. Observation of the inclined shear bands, which cause this local extremum of plastic strain ahead of the tip, draws a supposition that a Cottrell-type mechanism of microcrack nucleation at the intersection of the dislocation arrays (Knott [10]) may be operative there. As a complementary option, the micromechanism of fracture by slip band decohesion (Toribio and Kharin [11]), which was frequently associated with hydrogen effects in metals (Takeda and McMahon [12]), may also be involved. The other potential nucleus of microfracture is associated with stress-dominated micromechanism of fracture at maximum of the tensile stress σ_1 near the crack tip which is attained in another location $x_{c\sigma}$, see Fig. 1. The distance $x_{c\varepsilon}$ from the tip apex remains fairly constant when loading goes on. With specified model material and crack tip geometry, here $x_{c\varepsilon}$ is maintained at about 1-2 μm. The length $x_{c\sigma}$ increases whilst loading proceeds in a manner similar as described in other studies of the crack tip mechanics ([4-6], McMeeking [13]), roughly $x_{c\sigma} \propto K^2$. The extrema of the principal and the hydrostatic stresses σ_1 and σ are situated at fairly the same position $x_{c\sigma}$.

With regard to the load dynamics effect on the initiation of HAC, for subsequent comparisons let us consider first the sustained load test for which metal hydrogenation starts after a fixed load level, e.g. K_R, has been applied. On assuming that this level K_R corresponds to the threshold for HAC initiation, this means (Toribio and Kharin [14]), that criterion (1) may be fulfilled at the steady state equilibrium distribution of hydrogen in metal $C_e(x)$ being the thermodynamic maximum for a given sustained stress field $\sigma(x,K_R)$ shown in Fig. 1. The well known solution defines it for arbitrary hydrostatic stress as [1-3]

$$C_e(\sigma) = C_0 \exp \textbf{Fel!} \qquad (4)$$

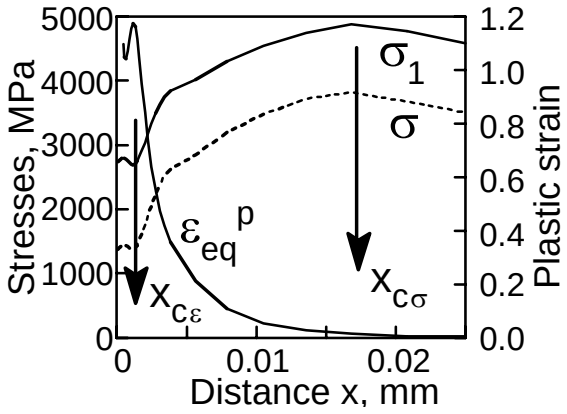

FIGURE 1. Equivalent plastic strain ε_{eq}^{p}, hydrostatic stress σ (in MPa) and maximum principal stress σ_1 ahead of the crack tip, depending on the distance from the tip apex in the deformed configuration during the rising load HAC test when applied load reaches K_R.

Depending on the dominating factor of microfracture —tensile stress or plastic strain— respective critical concentrations at $K = K_R$ may be evaluated according to the solution (4) and stress data displayed in Fig. 1 as $C_{cr\sigma}(\sigma_1) = C_e(x_{c\sigma},K_R) = 23.3C_0$ and $C_{cr\varepsilon}(\varepsilon_{eq}^{p}) = C_e(x_{c\varepsilon},K_R) = 3.24C_0$. The patterns of $C_e(x,K_R)$ are shown in Fig. 2.

Fig. 2 displays the coupled evolution of the stress-strain field and the hydrogen concentration in a fatigue pre-cracked specimen during rising load HAC test at $K^{\bullet} = 1.5$ MPa·m$^{1/2}$/min. At slower simulated loading with $K^{\bullet} = 0.15$ MPa·m$^{1/2}$/min the situation is basically the same, although concentration evolution followed closer after corresponding equilibrium distribution $C_e(K=K^{\bullet}\cdot t)$. The essential peculiarity of the dynamic HAC test in comparison with the sustained load one is that the position $x_{c\sigma}$ of the maximal tensile stresses (hydrostatic σ and principal σ_1) is not fixed, but moves deeper into the metal as load increases. When load rises not too fast, such as was modelled here with maximal $K^{\bullet} = 1.5$ MPa·m$^{1/2}$/min, this stress peak is able to erect and drag the accompanying peak of hydrogen concentration. In the course of loading, this peak passes the position $x_{c\varepsilon}$ of the potential strain-controlled fracture nucleus.

According to Figs. 2 and 3, the transient concentration $C(x_{c\varepsilon},t)$ temporarily becomes about twice the mentioned critical level $C_{cr\varepsilon}$ if the strain-dominated mode of hydrogen-assisted fracture were operative at sustained load and determined the critical concentration (1). This excessive hydrogenation at the strain concentration site $x_{c\varepsilon}$ occurs at substantially lower stress intensity factor $K \approx 0.15K_{IC} < K_R$, and this concentration surplus is maintained there during continuing loading up to attainment of the reference level of K_R (see Figs. 2 and 3). That is, approaching in a dynamic manner the crack tip situation when HAC may commence, local fracture event must occur at lower stress intensity factor than obtained in sustained load test, provided micromechanism of fracture is strain-controlled. This way, load dynamics may act as a promoter of HAC, which has been noted in some experiments, see review [14].

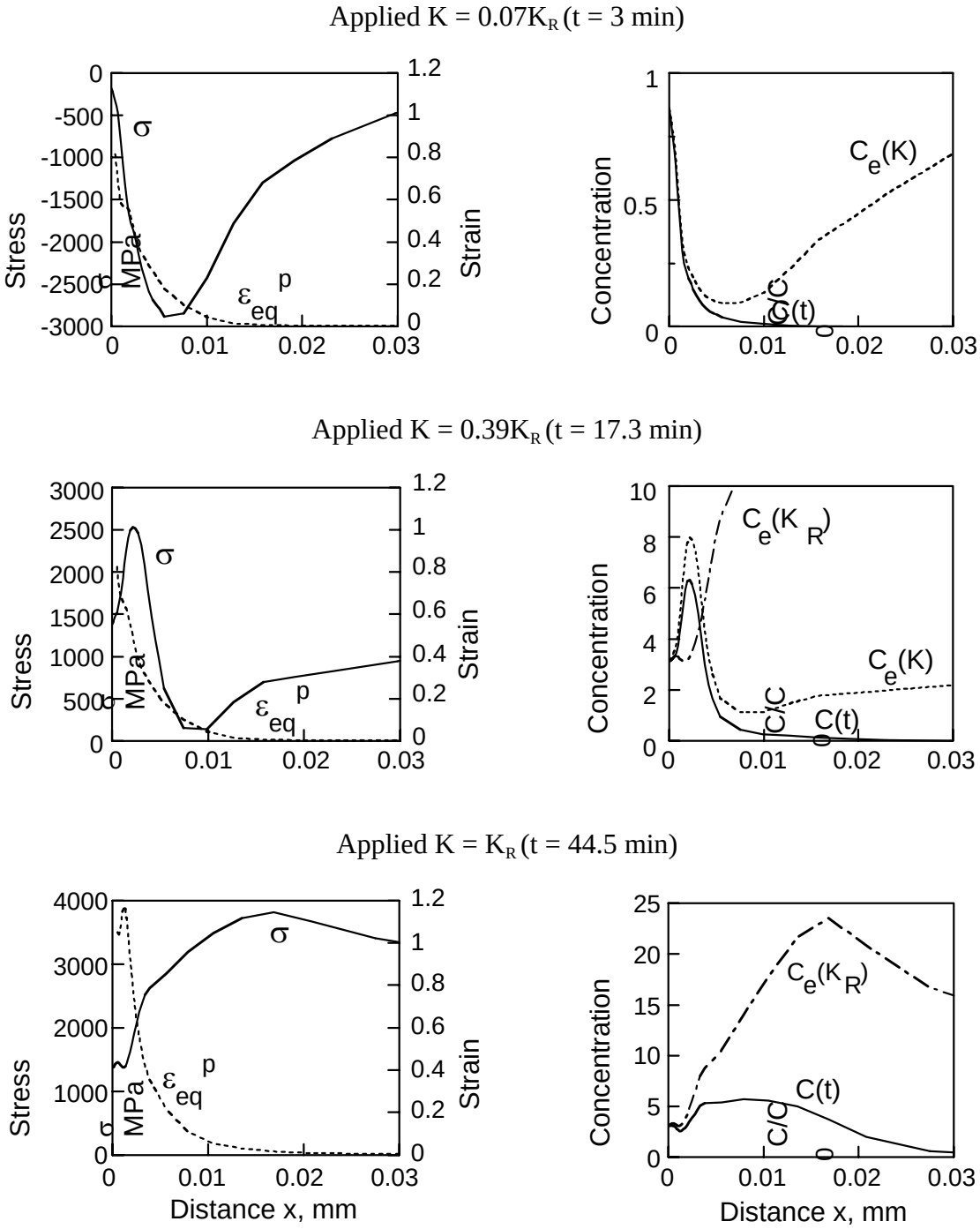

FIGURE 2. Sequence of distributions of the hydrostatic stress and equivalent plastic strain (left-hand column, solid and dotted curves respectively) and of hydrogen concentration (right-hand column, solid curve) in a fatigue pre-cracked specimen at indicated instants during the rising load HAC test at loading rate $K^{\bullet}$ = 1.5 MPa·m$^{1/2}$/min; for reference purposes, plots of the right-hand column also show the equilibrium concentration for the instantaneous stress field in the rising load test, $C_e(K=K^{\bullet}\cdot t)$, dotted line, and for the sustained load test at reference fixed load level K_R, $C_e(K_R)$, dashed-dotted line.

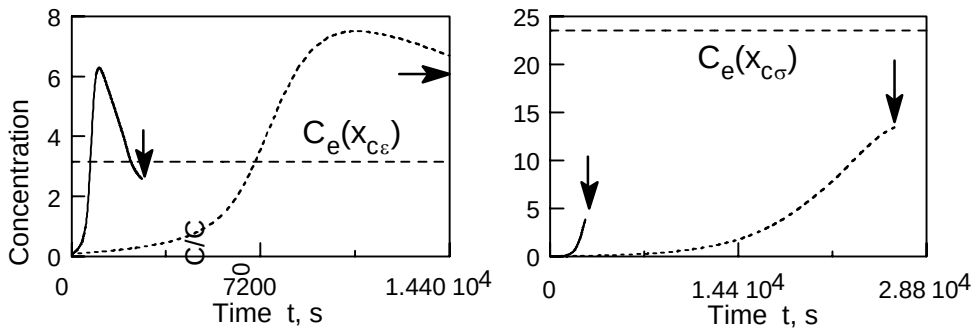

FIGURE 3. Concentration evolutions in the locations of possible strain- and stress-dominated local fracture, respectively $x_{c\varepsilon}$ (left-hand picture) and $x_{c\sigma}$ (right-hand graph), during dynamic HAC testing with the loading rates $K^{\bullet}$ = 1.5 and 0.15 MPa·m$^{1/2}$/min (solid and dashed curves, correspondingly); arrows indicate the moments of attainment of the reference load level K_R during the dynamic test and horizontal dashed lines mark the equilibrium concentration levels in respective locations under sustained load test at $K = K_R$, $C_e(x_c,K_R)$.

Described possibility of premature initiation of HAC due to dynamic loading cannot occur in the case of stress-controlled microfracture event. To provide the critical concentration $C_{cr\sigma} = C_{cr}(\sigma_1)$, cf. (1), at the maximum stress position $x_{c\sigma}$, applied loading must be slow enough to allow concentration to follow the evolution of the stress $\sigma(x_{c\sigma},t)$ with negligible delay, i.e., approximately maintaining the equilibrium concentration corresponding to the instantaneous stress field, $C(x_{c\sigma},t) \approx C_e(\sigma(x_{c\sigma},t))$ according to the steady-state solution (4). In the performed simulations the chosen loading rates are too fast to ensure this, as follows from Fig. 3, where concentration $C(x_{c\sigma},t)$ does not closely approach respective steady-state value up to the supposed threshold stress intensity level for HAC initiation K_R is attained. With less hydrogen accumulated till then, loading must proceed so that HAC initiates at higher level $K > K_R$ than under sustained load conditions. This corresponds to the frequently noticed experimental trend of diminishing of the harmful effect of hydrogen at faster load [14].

Described possibilities correspond to the limit cases of the general (and more realistic) fracture condition (1) according to which microfracture is governed by both stress and strain in a solid. In a more general case, critical cell location x_c must be somewhere between respective limit positions $x_{c\varepsilon}$ and $x_{c\sigma}$ in agreement with the typical patterns of the near tip stress-strain fields (Figs. 1 and 2). Obviously, this may produce a variety of manifestations in the matter of the effect of load dynamics on the susceptibility of metals to HAC.

Conclusions

Coupled simulations of the processes of elastoplastic deformation and stress-assisted hydrogen diffusion near the crack tip in the material with strain hardening under rising load were performed accounting for large deformations and residual stress-strain field generated by fatigue pre-cracking

Strain localisation caused by kinematic-type strain hardening was revealed, and it yielded discrimination of the separate possible nuclei of stress- and strain-controlled hydrogen assisted fracture. Comparing the conditions for HAC initiation from the point of view of the diffusional theory of hydrogen assisted fracture, it follows that load dynamics may act as a

promoter of HAC initiation when participation of the factor of (localised) plastic strain in the microstructural fracture mode is substantial.

Acknowledgements

The authors wish to thank the financial support of this work by the following institutions: Spanish Ministry for Scientific and Technological Research MCYT-FEDER (Grant MAT2002-01831), FEDER-INTERREG III (Grant RTCT-B-Z/SP2.P18), Junta de Castilla y León (JCYL; Grant SA078/04) and Spanish Foundation "Memoria de D. Samuel Solórzano Barruso". In addition, the authors wish to thank EMESA TREFILERIA S.A (La Coruña, Spain) for providing the steels used in the experimental programme.

References

1. Van Leeuwen, H.-P., *Engng Fract. Mech.*, vol. **6**, 141-161, 1974.
2. Toribio, J. and Kharin, V., *Nucl. Engng and Design*, vol. **182**, 149-163, 1998.
3. Toribio, J. and Kharin, V. *Fatigue Fract. Engng Mater. Struct.*, vol. **20**, 729-745, 1997.
4. Sofronis, P. and McMeeking, R. *J. Mech. Phys. Solids*, vol. **37**, 317-350, 1989.
5. Toribio, J. and Kharin, V., *Fracture From Defects. Proc. 12th European Conference on Fracture*, edited by M.W. Brown *et al*., EMAS, West Midlands, 1998, 1223-1228.
6. Toribio, J. and Kharin, V., *ASTM STP* **,** vol. **1343**, 440-458, 1999.
7. Toribio J. and Lancha A.M., *Mater. and Struct.*, vol. **26**, 30-37, 1993.
8. Kharin V., *Defect Assessment in Components. Fundamentals and applications*. ESIS/EGF Techn. Publ. 9, Mech. Engng. Publ., London, 1991, 489-500.
9. Panasyuk, V. and Kharin, V. *Environment Assisted Fatigue*. ESIS/EGF Techn. Publ. 7, Mech. Engng. Publ., London, 1990, 123-144.
10. Knott, J.F. *Fundamentals of Fracture Mechanics*, Butterworths, London, 1973.
11. Toribio, J. and Kharin, V., *Mater. Sci. Engng*, vol. **A234-236**, 575-578, 1997.
12. Takeda, Y. and McMahon, C.J., *Metall. Trans.*, vol. **12A**, 1255-1266, 1981.
13. McMeeking, R.M., *J. Mech. Phys. Solids*, vol. **25**, 357-381, 1977.
14. Toribio, J. and Kharin, V., *Physicochem. Mech. Mater.*, vol. **34** (4), 27-38, 1998.